DESIGNING A MOBILE ELECTROSPARK COATING SYSTEM FOR PRODUCING FUNCTIONAL SEMI-CONDUCTOR NANOPARTICLES

Feza Güngör, Turkey, fezagungor68@gmail.com

ARTICLE INFO

Gold medalist in BUCA IMSEF 2022

Awarded by Ariaian Young Innovative

Minds Institute , AYIMI

http://www.ayimi.org ,info@ayimi.org

ABSTRACT

In order to improve the standard electro-spark coating system, semiconductor metal oxide NPs; It was planned to design a control unit that controls the size distribution on the surface and provides limited accumulation to the linear region on the preferential axis. This control unit in the robotic platform provides the linear movement of the substrate in an axis during the spark, as well as the coaxial movement of the selected metal electrode pair. This project is considered to be successful in material production system design including robotic control unit, NP production and testing its effect on properties.

Key Words :*Electro-Spark Coating, Semiconductor,Robotic*

1. Introduction

The production of materials at the nanoscale enables the making of functional devices whose physical, chemical and biological properties can be changed and making these devices usable in our daily lives. Although composed of the same atoms, formations in different geometries create different material properties with different behaviors. This situation reveals how important the material production techniques can be, as it enables us to reach new and useful technologies.

Semiconductor metal oxide materials, on the other hand, arouse great interest in researchers working on nano-scale semiconductor devices, as they can be produced in various nanoscales, as well as being easy to manufacture. Moreover, these materials show unexpected properties when produced in different forms. For example, the optical and electrical properties of metals such as copper (Cu), gold (Au) are very different at the macroscopic and nanoscale. At the macroscopic scale, gold is yellow in color for its optical properties, but red at the nanoscale. Copper is opaque at the macroscopic scale (it absorbs more light) and quite transparent at the nanoscale. Bismuth, which has semimetal properties in macroscopic form, is semiconductor in nanowire form. The optical and electronic properties of materials vary greatly depending on their size. In that case, it will be possible to control many physical properties and functions of materials whose size can also be controlled.

The "moving electrospark coating system on robotic platform" designed in this project study and the translational movement of the substrate along a preferential axis during the spark, instead of the traditional "immobile substrate feature" in the coating technique, which is one of the plasma-based material preparation techniques, causes semi-metal oxide nanoparticle formation and physical effects on its properties were investigated.

In the standard electrospark coating technique, a high voltage difference is applied between two high purity metal electrodes, which are at a critical distance from each other. In this way, the spark formed between the electrodes vaporizes the electrode tips and metal particles are released. The next step is important from here. Because the process of depositing these metal particles on the substrate as metal oxide nanoparticles by combining with the oxygen in the atmosphere is the reason for the emergence of this project. Since the subject of our interest is the production of semiconductor metal oxides, it is very important to be able to deposit the resulting NPs into the desired template area. Thus, a more comfortable working area will be created on a suitable surface for applications such as diodes and sensors.

In this study, one of the most important parameters in the semi-metal oxide nanoparticle generation system is the size of the electrostatic energy stored in the capacitor. Capacitor energy is highly dependent on the voltage difference between metal electrodes. When capacitor energy is released, direct current (dc) creates a high temperature plasma arc between the ends of the two electrodes. In the examination of the NP production system and the resulting product material, separate experiments should be carried out for certain values of the voltage difference between the electrodes. This process is necessary because, depending on the magnitude of the voltage difference applied between the electrodes, there are differences in the shapes of the nanoparticles deposited on the substrate surface.

It is possible to create many properties and application areas by succeeding in controlling the structure of semiconductor nanoparticles. Therefore, an interface design was carried out to control the size distribution of the semiconductor metal oxide NP and to be linearly oriented and deposited to a preferential region. This interface gives the substrate an axial movement capability controlled by Arduino UNO, and it produces NPs for different spark voltage values at certain intervals, at once, with the systematic movement of the substrate. Accumulation of nanoparticles at the desired line length and concentric smooth placement on the target area on the substrate surface in one go, on the preferential axis, has been successfully achieved. The interface designed in this study works as a functional robotic control component that performs both operations at the same time and enables NPs to be deposited into millimetric or micro channels (template). Since the same component moves the substrate during spark, NP production is provided in independent, parallel and linear channels (template) on the substrate surface, and it is possible to cover the substrate surface with

homogeneous semiconductor nanoparticle channels. The critical element in this process; It is the accumulation of nanoparticles in a homogeneous and preferential region of the substrate surface with identical dimensions. If the homogeneous distribution of nanoparticles on the substrate surface and size control cannot be achieved, effective optical and electrical properties cannot be achieved. Therefore, the most important feature of this robotic component is to create electronic and/or electrooptical paths on suitable surfaces.

It covers measurement systems that will determine the application areas. Once it is understood that the properties of materials change depending on their size, they are very valuable for many application areas such as electronics, computers, aviation, space, health, energy, defense and food. There are various studies on the antimicrobial properties of gold and silver NPs (Singh et al., 2014; Habiboallah et al., 2014; Nambiar et al., 2010) to ZnO (zinc oxide) NPs on their capacity to act as gas sensors (Singh et al., 2010). ., 2014). The fact that nanoscale materials are lighter, more robust, and programmable means that the same or more processes can be performed with less material compared to large-size material. This also means less energy, cost and hassle.

There are different techniques to produce materials at the nanoscale. These are generally material preparation techniques created in solution, plasma or vacuum systems (Rane et al., 2008). Plasma-based techniques are frequently used to produce materials such as particles and wires at nanoscale. Electro-spark also; It is a technique with different arc capacity depending on the type of electrodes used, cross-sectional area and work function. Although it is a very simple technique, the cost for the needs may vary. After the first studies for the purpose of producing materials, applications were made in the normal atmosphere environment without the need for vacuum (Schwyn et al., 1988). In various researches, this technique; carbon nanoparticles (Horvath et al., 2003), carbon flakes (Tabrizi et al., 2009), metals (Tabrizi et al., 2010), metal oxide nanoparticles (Kim et al., 2005; Vons et al. , 2011), semiconductor nanoparticles, Si nanoparticles (Kumpika et al., 2008), Zinc-Oxide nanoparticles (Güngör et al., 2017), Copper-Oxide nanoparticles (Güngör and akd., 2019).

In this study, it is aimed to increase the capacity of the system to be used in semiconductor nanomaterial production and semiconductor device applications by adding interfaces such as robotic control unit to a standard electrospark coating system. Thus, the mobile electrospark coating system was installed on the robotic platform, the details of which are given in the "Methods" section, and thin films consisting of nanomaterials produced with this system were examined optically, surface and electrically.

2. Materials and Methods

In this study, the system designed to produce functional semiconductor metal oxide NP basically consists of two main units. The first is the robotic control unit that simultaneously provides the axial movement of the substrate controlled by the Arduino UNO and the concentric movement of the metal electrode pair. The other is the high voltage unit used to create the plasma-based arc between the electrodes.

High voltage unit; It consists of a variac that provides 0-220V output and a DC high voltage source whose output voltage can be adjusted between 0-6kV, the capacitor used to store energy and the switch used to adjust the spark number (Fig.1a). Here, the 0.2 µF/5kV capacitor is charged with a voltage difference of 3kV, 4kV and 5kV, and the stored 0.9J, 1.6J and 2.5J electrical energy is discharged between the electrodes. High purity Zn, Ag and Cu electrodes were used in the experiments. Spark speed is set to be 1 every 3s. Thin film sample group consisting of each semi-metal oxide nanoparticle was prepared with a spark number of 10. Microscope glass was used as substrate. The position of the metal electrodes is adjusted relative to the horizontal axis. The vertical axis distance between the glass substrate and the metal electrodes is approximately 1 mm.

The robotic control unit, on the other hand, has two freedoms of movement at the same time. One of them is related to the axial movement of the substrate during the spark. Axial movement was controlled by microcontroller (Arduino Uno) and step-motor driver unit with the values determined by the user for the number of steps. For this control process, in addition to the micro-step feature and 1, 2, 4, 8, 16 and 32 steps, the pitch value of the mechanical system is taken into account. In this way, the linear regions (lines) on which nanoparticles are coated on the substrate surface are separated from each other. Another feature of the robotic control unit is that it can provide planar motion control not only in one axis, but also in both axes for a fixed spark voltage value (Fig.1b). Thanks to this feature, it will be possible to produce devices such as optical and electrical circuit elements by coating semiconductor nanoparticles on special template surfaces. The other motion controlled by the robotic unit is related to the concentric motion of the metal electrode pair. In concentric motion, it was decided to use an intermediate element (M8X1) with metric-8 right and left threads to control the distance between metal electrodes and combined with a second step-motor driver unit with Arduino Uno. Thus, the step-motor completes 1.8 degrees with different steps (up to 6400 steps), which are multiples of 2. It is possible to control the distance between the electrodes in the order of 10-6m. The schematic representation of the rsystem designed and used in the project is given in Figure (1c).

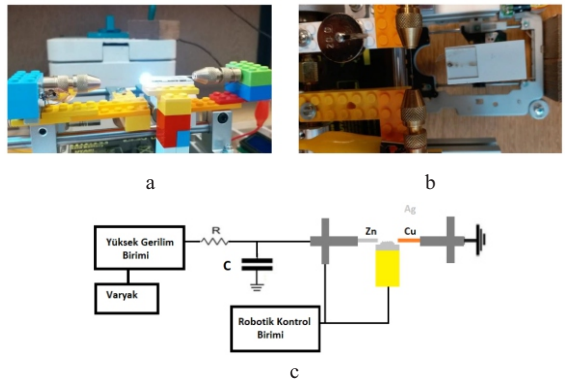

Fig. 1: Photographs taken during electro-sparking in the nanoparticle deposition system (a) and during the movement of the substrate with a single axis robotic control unit (b), Schematic representation of the system (c)

In order to examine the optical properties of semiconductor metal oxide nanoparticles produced with the system controlled by Arduino UNO-based, optical transmittance spectra in the wavelength range of 300-1100 nm were obtained at room temperature. For this, a UV-Vis spectrophotometer (Seeman 3000) with CCD (Charge Coupled Device) detector was used. Experimental optical transmittance spectra of thin films in the uniaxial linear region where semi-metal oxide nanoparticles accumulate

on the substrate were obtained. The optical constants of the material (such as film thickness, refractive index, optical band gap) cannot be obtained directly from the experimental optical transmittance spectra obtained in a certain wavelength range. Therefore, theoretical spectrum curves obtained by calculation are fitted to the experimental spectrum by means of utilities in the computer environment. In this study, the program that provides us this convenience is a computer program that works on the basis of the unconstrained minimization algorithm by Birgin (Birgin et al., 1999). In this way, theoretical optical transmittance spectra, which give the best agreement with the experimental optical transmittance spectra, were obtained. Then, information such as film thickness, refractive indices, optical band gap of the samples were obtained from these theoretical spectra. Scanning electron microscope (SEM, FEI Quanta FEG 250) was used to examine the surface properties and energy dispersive spectroscopy (EDS, Energy Dispersive Spectroscopy) analyzes were used to determine atomic concentrations. Electrical measurements; were made using 4-point technique for Ag doped ZnO and Cu doped ZnO samples at room temperature. For this, an optical microscope (USB connection, x1000) and current-voltage unit were used to observe the movement of these types at the micrometer scale during the measurement with two tungsten types (Fig. 2 a, b and c).

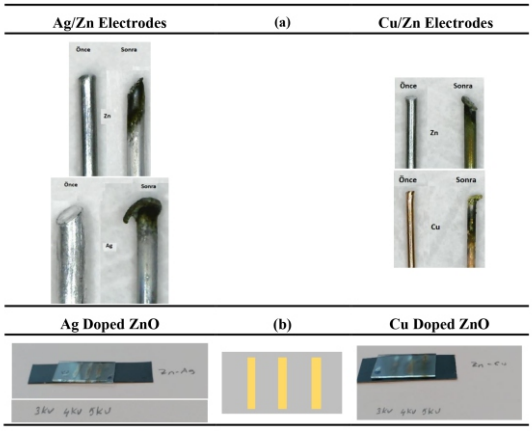

Fig. 2: Photographs of Ag/Zn and Cu/Zn metal electrodes before and after electro-spark (a) and photographs of thin-film samples formed from Ag-doped ZnO and Cu-doped ZnO nanoparticles obtained with the rHESK system, and schematic representation showing the linear sample regions on the substrate surface (b)

The experimental optical transmittance spectra of the samples produced for each different spark voltage in the system are shown in Figures (3) and (4). Accordingly, the Cu-doped ZnO nanoparticle thin film formed with 4kV spark voltage is highly optically permeable, that is, quite good transparent, compared to the samples obtained for other spark voltages. The Cu-containing sample obtained when 3kV spark voltage is applied is not sufficiently optically permeable compared to the other samples in this group. However, Ag-doped ZnO samples showed high optical transmittance for the wavelength of the light used in optical transmittance measurements greater than 550nm.
The graphs in Figures (5) and (6) show the theoretical spectra of Ag-doped ZnO and Cu-doped ZnO thin films obtained when a spark voltage of 4kV is applied between the electrodes, which is consistent with the experimental optical transmission spectra. Just like the experimental optical transmittance spectra obtained for each sample separately, the theoretical optical transmittance spectra for each sample were obtained separately.

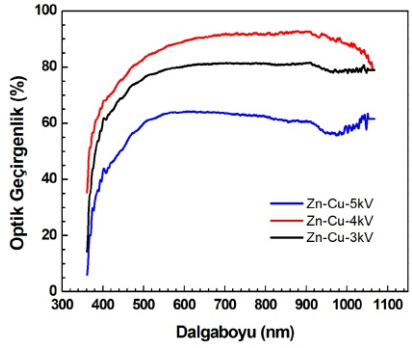

Fig. 3: Experimental optical transmission spectra of thin films of Cu-Zn-Oxide nanoparticles obtained with Cu/Zn metal electrode pair for different spark voltages.

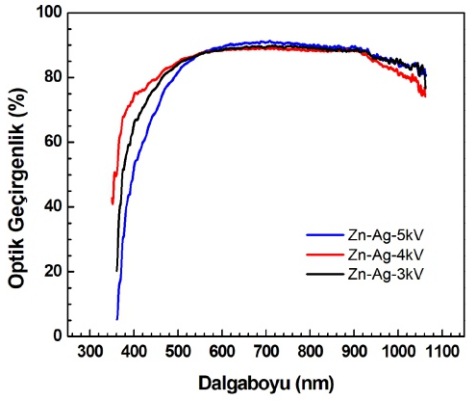

Fig. 4: Experimental optical transmission spectra of thin films composed of Ag-Zn-Oxide nanoparticles obtained with Ag/Zn metal electrode pair for different spark voltages

The film thicknesses and optical band gaps determined by using these spectra obtained for three different spark voltages of the Ag-containing and Cu-containing ZnO sample groups are given in Table (1). From this information, it was observed that the optical band gap in both Cu-containing and Ag-containing metal oxide NP sample groups increased with spark voltage. The thickness of the thin films formed by nanoparticles varies in the range of 74-196nm.

Table 1: Parameters of metal oxide nanoparticles produced with the system designed in the project. Thickness t, optical band gaps Eg, average NP size D and electrical resistances of elements obtained from EDS analyzes R of thin film samples formed from nanoparticles obtained for different spark voltages

Elektrot Couples	Sample	V_{spark} (kV)	t (nm)	E_{gap} (eV)	D (nm)	Ag amount (%)	Cu amount (%)	Zn amount (%)	R (kΩ)
Ag/Zn	Ag-ZnO	5	181	3.1630	50	0.05	--	2.78	33
		4	196	3.0700	60	0.05	--	2.52	12
		3	183	3.0600	60	0.18	--	5.41	56
Cu/Zn	Cu-ZnO	5	95	3.1045	20	--	0.38	3.05	4000
		4	74	3.0780	70	--	0.30	3.97	8000
		3	174	3.0580	60	--	1.04	1.52	12000

SEM images of the samples obtained with Ag/Zn and Cu/Zn electrode pairs in the rHESK system, depending on the spark voltage values (5kV, 4kV and 3kV), are shown in

in Figures (7) and (8).

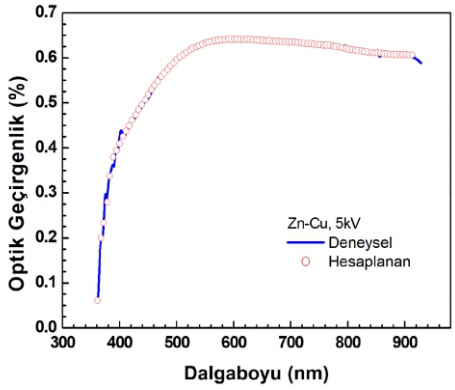

Fig. 5: Experimental (-) and theoretical (o) optical transmittance spectra of thin film consisting of Cu-Zn-Oxide nanoparticles obtained with Cu/Zn metal electrode pair for 5kV spark voltage

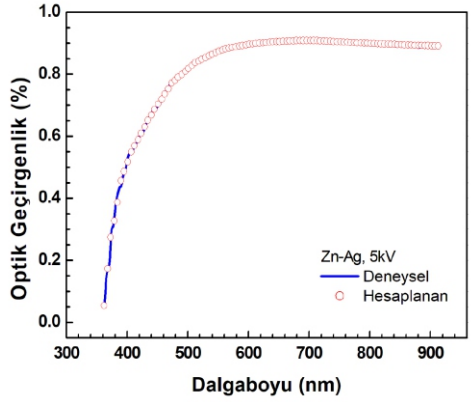

Fig. 6: Experimental (-) and theoretical (o) optical transmittance spectra of thin film consisting of Ag-Zn-Oxide nanoparticles obtained with Ag/Zn metal electrode pair for 5kV spark voltage

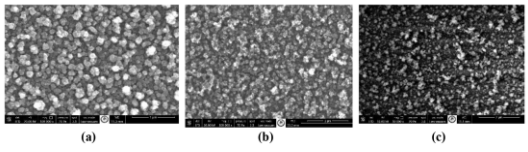

Fig. 7: SEM images of Ag-Zn-Oxide nanoparticle films obtained with Ag/Zn electrode pair for spark voltages of 5kV (a), 4kV (b) and 3kV (c)

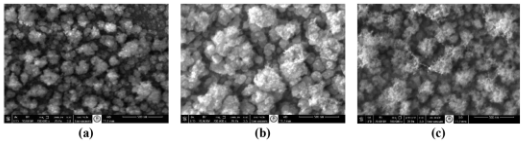

Fig. 8: SEM images of Cu-Zn-Oxide nanoparticle films obtained with Cu/Zn electrode pair for spark voltages of 5kV (a), 4kV (b) and 3kV (c)

When 5kV spark voltage is applied to Ag/Zn electrodes, groups with an average diameter of 60nm and groups with diameter distribution in the 40-230 nm range, which can be distinguished from each other, were observed. When 4kV spark voltage is applied, NPs of 30-80nm dimensions were observed. While an average NP size of 60nm was observed in the sample obtained when 3kV spark voltage was applied, it was observed that NPs overlapped (agglomeration) in places.

When 5kV spark voltage was applied to Cu/Zn electrodes, the lowest 20 nm NPs were observed, while pellets with an average diameter of 180 nm were also observed due to overlapping NPs. When 4kV spark voltage was applied, the average NP size was determined as 70nm and the NPs were more evenly distributed on the surface. In the sample produced with 3kV spark voltage, a fringed formation formed by nanowires and NPs of different lengths and approximately 10nm in width was observed.

SEM images made us think of other possibilities. The work-functions of the electrodes used during the sparking process (4.33eV for Zn, 4.26 eV for Ag and 4.65 eV for Cu) are different from each other. Due to the high energy values stored in the capacitor with high spark voltages and the high kinetic energies gained by the nanoparticles formed while discharging during the arc, it is considered that NPs may jump to different positions on the substrate surface or, if they are lower, may not complete the nanoparticle shaping, adhere to the surface or clump. The elemental analysis values of the EDS measurements made by selecting a specific region on the surfaces of the samples produced with Ag/Zn and Cu/Zn electrode pairs are shown in Table 1. In Figures (9) and (10), EDS spectra of Ag-containing and Cu-containing ZnO samples produced with 4kV spark voltage are shown as examples. In these analyzes, it was understood that Ag ions entered the ZnO structure in a very small amount, but Cu ions relatively more. The electrical measurement results are shown in Table (1). The electrical resistances of Cu-containing ZnO samples in the order of M decrease as the spark voltage increases. Ag-containing ZnO samples, on the other hand, have resistances of the order of k, the resistance values change depending on the amount of Ag ions in the ZnO structure.

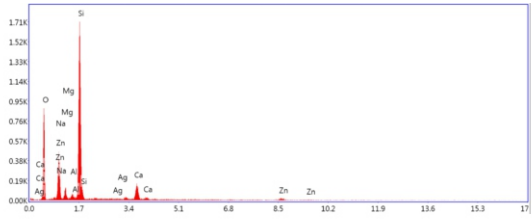

Fig. 9: EDS analysis of a thin film sample consisting of Ag-Zn-Oxide nanoparticles for 4kV spark voltage with Ag/Zn electrode pair

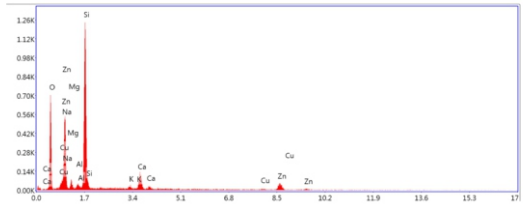

Fig. 10: EDS analysis of the film sample consisting of Cu-Zn-Oxide nanoparticles for 4kV spark voltage with Cu/Zn electrode pair

3. Conclusin and Discussions

New technologies are required to produce materials at the nano-scale and to study their properties. In this project study, the standard electrospark coating system, which is a plasma-based material preparation technique in which nanomaterials such as nanoparticles and nanowires can be prepared, was developed to produce functional semiconductor nanoparticle structures that can be used as a

device, its applications were made and its physical properties were examined. Therefore, the project studies were planned in three main groups.

The first group; It includes the design and installation of the material production system and the software of the robotic control unit. In the standard electrospark coating system, the substrate surface on which the nanomaterial will be coated is immobile, and the nanoparticles that emerge thanks to the spark between the electrodes accumulate on the substrate surface. Physical properties of materials; Since it changes according to the size, shape and arrangement on the surface, designs were made to ensure the formation of homogeneous semiconductor paths on the substrate surface, and the first prototype of a new electrospark coating system called sHESK emerged. The second group of work; involves the production of semiconductor nanomaterials. With the designed system, Ag doped ZnO and Cu doped ZnO samples were produced. By applying different spark voltages with this system, the formation of independent, parallel, linear regions consisting of semiconductor nanoparticles on the substrate surfaces has been successfully achieved.

Last group work; It includes the examination of the physical properties of the produced samples. The Cu-doped ZnO nanoparticle thin film produced with 4kV spark voltage is highly optically permeable compared to the samples obtained for other spark voltages. Ag-doped ZnO samples, on the other hand, showed high optical transmittance for the wavelength of the light used in optical transmittance measurements greater than 550nm.

Thicknesses of thin films formed by Cu-containing and Ag-containing metal oxide nanoparticles vary in the range of 74-196nm. In both sample groups, the optical band gap increases with the spark voltage. It has been observed that the nanoparticle sizes vary in the average range of 20-70nm. In sample structures from SEM images; In addition to nanoparticle forms, it has been observed that nanowire forms are also formed. In the test experiments carried out according to the EDS analysis, it was understood that Ag ions entered the ZnO structure in very small amounts, but Cu ions relatively more. The electrical measurement results showed that Cu-containing ZnO samples had resistances in the order of M, while Ag-containing ZnO samples had resistances in the k order.

In this project work; Optical, surface and electrical properties of thin film materials obtained with Ag-containing and Cu-containing ZnO nanoparticles were investigated depending on the spark voltage values between the electrodes. In these experiments, the spark number and the translational velocity of the substrate were kept constant. In the rHESK system, which was developed for the production of nanoparticles and other forms, it was observed that nanoparticle sizes, shapes, and therefore optical and electrical properties can be changed by changing the spark voltage, spark number and substrate velocity in the first place. Physical properties can be controlled with rHESK system parameters and these semiconductor films made of metal oxide nanoparticles; It can be used in the construction of devices such as LED, solar cell, diode, sensor, varistor, capacitor. These devices can be evaluated in many areas such as space, energy, defense, health and food.

4. Suggestions

The designed rHESK system can also be used by planning different nanomaterial production parameters apart from the works within the scope of the project. In the system used in the atmosphere, the area where the arc occurs can be closed and the surface coating experiments can be repeated with electrospark in an appropriate and inert (non-reacting) gas environment. By using different substrate surfaces, substrates with different surface energies can be coated with metal oxide nanoparticles. Because the adhesion of an energetic particle to every solid surface does not occur under the same conditions. The effect of substrate on nanoparticle formation can be investigated.

Acknowledgements

In this study, photographs of the physical changes of Zn, Ag and Cu metal electrodes in the system before and after electro-spark are given in Figure 2 (a). Wear, melting and sedimentation were observed at the ends of the metal electrodes after electro-sparking. Photographs of thin film samples consisting of metal oxide nanoparticles formed on the glass substrate surface are shown in Figure 2(b). In these photographs, it is seen that independent, parallel, semiconductor linear regions consisting of Ag doped ZnO and Cu doped ZnO nanoparticles form on the substrate surfaces.

References

[1] Birgin, E.G., Chambouleyron, I., Martinez, J.M. (1999). Estimation of the optical constants and the thickness of thin films using unconstrained optimization, Journal of Computational Physics, 151(2), 862-880. doi:10.1006/jcph.1999.6224.

[2] Greiner, M., Lu, ZH. (2013). Thin-film metal oxides in organic semiconductor devices: their electronic structures, work functions and interfaces. NPG Asia Mater 5, e55. doi:10.1038/am.2013.29.

[3] Güngör, E. Güngör, T, Çalışkan, D. Özbay, E. (2019). Cu Doping Induced Structural and Optical Properties of Bimetallic Oxide Nanodots by the Vertical Spark Generation, Acta Physica Polonica A,135(5), 857-862. doi:10.12693/APhysPolA.135.857.

[4] Güngör, E. Güngör, T, Çalışkan, D. Özbay, E. (2017). Synthesis and optical properties of Co and Zn-based metal oxide nanoparticle thin films, Acta Physica Polonica A, 131(3), 500-503. doi: 10.12693/APhysPolA.131.500.

[5] Habiboallah, G., Mahdi, Z., Majid, Z., Nasroallah, S., Taghavi, A.M., Forouzanfar, A., & Arjmand, N. (2014). Enhancement of Gingival Wound Healing by Local Application of Silver Nanoparticles Periodontal Dressing Following Surgery: A Histological

[6] Assessment in Animal Model. doi:10.4236/MRI.2014.33016

[7] Horvath, H., Gangl, M. (2003). A low-voltage spark generator for production of carbon particles, Journal of Aerosol Science, 34, 1581-1588. doi:10.1016/S0021-8502(03)00193-9.

[8] Kim, J.T., Chang, J.S. (2005). Generation of metal oxide aerosol particles by a pulsed spark discharge technique, Journal of Electrostatics, 63, 911-916. doi:10.1007/s11051-008-9407-y.

[9] Kumpika, T., Thongsuwan, W., Singjai, P. (2008). Optical and electrical properties of ZnO nanoparticle thin films deposited on quartz by sparking process, Thin Solid Films, 516, 5640-5644. doi:10.1016/j.tsf.2007.07.062.

[10] Nambiar, D., & Bhathena, Z. P. (2010). Use of silver nanoparticles from Fusarium oxysporum in wound

dressings. Journal of Pure and Applied Microbiology, 4(1), 207-214.

[11] Rane, A.V., Kanny, K., Abitha, V.K., ve Thomas, S. (2018). Synthesis of Inorganic Nanomaterials, Methods for Synthesis of Nanoparticles and Fabrication of Nanocomposites. Synthesis of Inorganic Nanomaterials içinde (121–139). Woodhead Publishing. doi:10.1016/b978-0-08-101975-7.00005-1.

[12] Schwyn, S., Garwin, E., Schmidt-Ott, A. (1988). Aerosol Generation by Spark Discharge, Journal of Aerosol Science, 19, 639-642. doi: 10.1016/0021-8502(88)90215-7.

[13] Singh, R. and Sing, D. (2014). Chitin membranes containing silver nanoparticles for wound dressing application, International Wound Journal, 11(3), 264-268. doi: 10.1111/j.1742-481X.2012.01084.x

[14] Singh, A. K. Rapid and eco-friendly synthesis of copper nanoparticles, AIP Conference Proceedings, 1591 (1) (2014) 372-373. doi:10.1063/1.4872606

[15] Tabrizi, N.S., Ullmann, M., Vons, V.A., Lafont, U., Schmidt-Ott, A. (2009). Generation of nanoparticles by spark discharge, Journal of Nanoparticle Research, 11, 315-332. doi:10.1007/s11051-008-9407-y.

[16] Tabrizi, N.S., Xu, Q., van der Pers, N.M., Schmidt-Ott, A. (2010). Generation of mixed metallic nanoparticles from immiscible metals by spark discharge, Journal of Nanoparticle Research, 12, 247-259. doi:10.1007/s11051-009-9603-4.

[17] Vons, V.A., de Smet, L.C.P.M., Munao, D., Evirgen, A., Kelder, E.M., Schmidt-Ott, A. (2011). Silicon nanoparticles produced by spark discharge, Journal of Nanoparticle Research, 13, 4867-4879. doi:10.1007/s11051-011-0466-0.